

Fabrication and characterization of TiO₂ nanotube arrays on Ti membrane enlarged by anodic oxidation

JONG-OH KIM¹, CHRUL-HEE CHO², WON-YOUL CHOI^{3,4*}

¹Department of Civil and Environmental Engineering, Hanyang University, Seoul 131-791, Korea

²Graduate School of Green Energy Technology, Chungnam National University, Daejeon 305-764, Korea

³Department of Metal and Materials Engineering, Gangneung-Wonju National University, Gangneung 210-702, Korea

⁴Research Institute for Dental Engineering, Gangneung-Wonju National University, Gangneung 210-702, South Korea

TiO₂ nanotube arrays have attracted a great deal of attention as photocatalytic and photoelectrode materials due to their large surface area, low cost and easy fabrication. Highly ordered TiO₂ nanotube arrays for the photoelectrodes in dye-sensitized solar cells have been fabricated from Ti foil. However, the TiO₂ nanotube arrays from Ti foil were not effective for the photocatalytic materials, because it had only one plane for the photocatalytic reaction. We have fabricated the TiO₂ nanotube arrays from macroporous Ti metal membrane by anodic oxidation and tried to scale it up. Various factors were controlled to obtain the optimal microstructure of the TiO₂ nanotube arrays on the surface of macroporous Ti metallic membrane. Microstructure and phase were studied by SEM and XRD, respectively. Temperature was a very important factor in anodic oxidation of large surface area. 10 μm thick TiO₂ nanotube arrays on Ti metallic membrane having a large surface area were fabricated and some factors for scaling-up were discussed.

Keywords: *TiO₂ nanotube arrays; anodic oxidation, photocatalysis; scaling-up; anatase*

© Wrocław University of Technology.

1. Introduction

TiO₂ is known to be the most effective photocatalyst, and photocatalytic degradation using TiO₂ is one of the most promising methods to eliminate the refractory organic contaminants in water and wastewater [1–6]. TiO₂ materials make it possible for the organic contaminants to be easily removed at ambient temperature and pressure [7–10]. The coupling of TiO₂ photocatalytic reaction with membrane separation process can take advantage of the synergy of both technologies. Utilization of UV radiation coupled with TiO₂ can also enhance the oxidizing power to remove the organic contaminants [11, 12]. However, the use of TiO₂ nanoparticles as photocatalysts in aqueous suspensions is limited in commercial applications because the separation process for TiO₂ nanoparticles is additionally required. To avoid the additional process,

considerable work has been performed to develop immobilized TiO₂ nanoparticles on various substrates, such as thin films and membranes [13–15]. The photocatalytic activity of immobilized TiO₂ nanoparticles is low due to exfoliation of the deposited TiO₂ thin film and because of reduction of the effective surface area that is to be illuminated [16].

TiO₂ nanotube arrays have attracted much attention because of their large specific surface area for the photocatalytic reaction [17, 18]. There is no need to separate TiO₂, because TiO₂ nanotube arrays are grown on the Ti metallic substrate [14, 19–22]. TiO₂ nanotube arrays on Ti metallic substrate have been studied for photocatalytic degradation of organic contaminants [14, 23–26]. Ti metallic membrane with macroporous structure can allow water to flow through the membrane.

In this work, Ti metallic membrane with macroporous structure was selected to improve the permeability of water and photocatalytic efficiency

*E-mail: cwy@gwnu.ac.kr

of TiO₂. TiO₂ nanotube arrays were grown on the surface of Ti metallic membrane by anodic oxidation. Various areas of Ti metallic membrane were anodized for practical applications. In anodic oxidation of large Ti metallic membrane, scaling-up factors, such as temperature and transient current, were discussed. Microstructure and phase of TiO₂ nanotube arrays were studied by SEM and XRD, respectively.

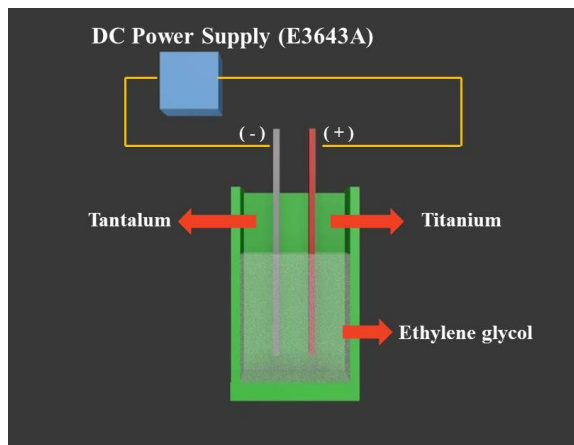


Fig. 1. Schematic diagram of anodic oxidation system for large scale Ti metallic membrane.

2. Experimental

TiO₂ nanotube arrays were fabricated by anodic oxidation of 1.0 mm thick Ti metallic membrane (~98 %, Xinxiang Xinli Purification Tech. Co., Ltd.) in ethylene glycol solution containing 0.3 wt.% NH₄F and 2 vol.% H₂O. Anodic oxidation was conducted at a constant potential with a DC power supply (E3643A, Agilent Technologies, Inc., USA). Current variation during anodization was monitored using a digital multimeter (34401A, Agilent Technologies, Inc., USA). The DC power supply and digital multimeter were computer-controlled by GPIB interface and LabVIEW program. A constant potential of 60 V or 20 V with a ramping speed of 1 V/s was applied between the anode and the cathode. Tantalum was used as a counter electrode. Fig. 1 shows a schematic diagram of anodic oxidation system for large scale Ti metallic membrane. After anodic oxidation, TiO₂

nanotube arrays were rinsed with DI water and annealed at 500 °C for 1 hour for the phase transformation. The pore size, wall thickness, and length of TiO₂ nanotube arrays were determined by field emission scanning electron microscopy (FE-SEM, Philips XL 30SFEG) at Korea Basic Science Institute. Annealed TiO₂ nanotube arrays were analyzed by XRD (X-ray diffractometry, Rigaku D/MAX-RC, CuK α radiation). For anodic oxidation of large Ti metallic membrane, various areas, such as 2 × 3 cm², 3 × 3 cm², 10 × 10 cm², 12 × 15 cm², were selected and anodized. Temperature was controlled during anodic oxidation. Transient currents measured by digital multimeter (Agilent 34401A) were monitored.

3. Results and discussions

Microstructure of Ti metallic membrane was observed by FESEM. Fig. 2a and 2b show the plane views of Ti metallic membrane before anodic oxidation at low magnification and high magnification, respectively. There are macropores, and water with organic contaminants flow through the macropores. The path of water through the macropores is very long and it can provide a sufficient time for photocatalytic reaction. After anodic oxidation, highly ordered TiO₂ nanotube arrays were obtained on the surface of Ti metallic membrane. Fig. 2c and 2d show FESEM images of TiO₂ nanotube arrays fabricated by anodic oxidation in ethylene glycol solution containing 0.3 wt.% NH₄F and 2 vol.% H₂O. Anodizing voltage and time were 60 V and 20 min, respectively. To compare the top image of Ti metallic membrane before anodic oxidation with that after anodic oxidation, a part of Ti metallic membrane was masked and anodized. Fig. 2c shows the top image of Ti metallic membrane before and after anodic oxidation at once. TiO₂ nanotube arrays and TiO₂ nanotubes are hexagonally close-packed together. The very clean and open TiO₂ nanotube arrays are observed. Their pore size, tube diameter, and wall thickness are ~80 nm, ~120 nm, and ~20 nm, respectively. The thickness of TiO₂ nanotube arrays is ~10 μ m. Some cracks on the surface of Ti metallic membrane resulting from the difference of thermal expansion coefficients between

TiO₂ nanotube arrays and Ti metallic membrane are observed.

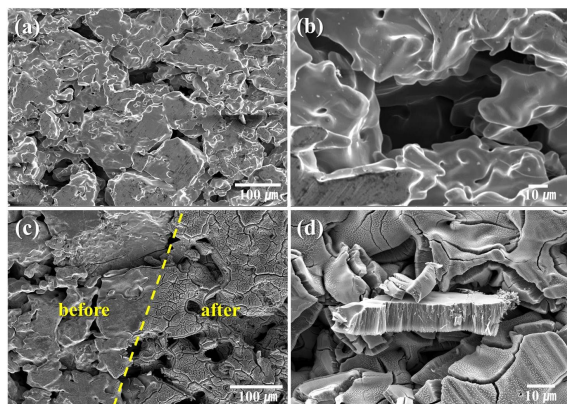


Fig. 2. FESEM images of Ti metallic membrane before anodic oxidation: (a) top view of TiO₂ nanotube arrays before anodic oxidation at low magnification, (b) top view of TiO₂ nanotube arrays before anodic oxidation at high magnification, (c) top view of TiO₂ nanotube arrays after anodic oxidation at low magnification, (d) top view of TiO₂ nanotube arrays after anodic oxidation at high magnification.

To investigate scale-up factors in anodic oxidation, four sizes of samples, i.e. 2 × 3 cm², 3 × 3 cm², 10 × 10 cm², and 12 × 15 cm² were prepared. These samples were anodized with anodizing voltage of 20 V in ethylene glycol solution containing 0.3 wt.% NH₄F and 2 vol.% H₂O. When anodizing voltage of 60 V was applied to the sample of 12 × 15 cm², the transient current was dramatically increased and the current was higher than 1 A. Lower voltage of 20 V was selected to avoid an electric shock. Fig. 3 shows FESEM images of TiO₂ nanotube arrays obtained from Ti metallic membranes with the size of 2 × 3 cm², 3 × 3 cm², 10 × 10 cm², and 12 × 15 cm², respectively. TiO₂ nanotube arrays are similar to those grown by anodic oxidation at 60 V. Surface morphology of TiO₂ nanotube arrays obtained at 20 V is less clean than that obtained at 60 V.

Anatase in various TiO₂ crystalline phases has been reported as the best phase for photocatalytic reaction. To obtain anatase TiO₂ nanotube arrays, as-anodized TiO₂ nanotube arrays were annealed. Fig. 4 shows X-ray diffraction (XRD) spectrum of

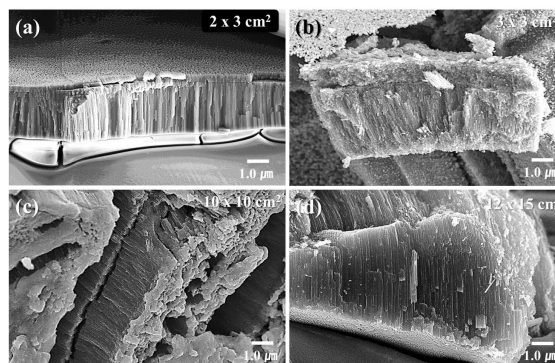


Fig. 3. FESEM images of TiO₂ nanotube arrays obtained from Ti metallic membrane with various areas: (a) 2 × 3 cm², (b) 3 × 3 cm², (c) 10 × 10 cm², (d) 12 × 15 cm².

TiO₂ nanotube arrays on Ti metallic membrane annealed at 500 °C for 1 h. Anatase peaks are shown together with Ti metal peaks in Fig. 4. Anatase peaks at 2-theta near 25°, 37°, 38°, 47°, 54°, and 55° are observed. Titanium metal peaks originate from the Ti metallic membrane as a substrate. XRD patterns reveal that TiO₂ nanotube arrays were successfully crystallized into the anatase phase by annealing at 500 °C.

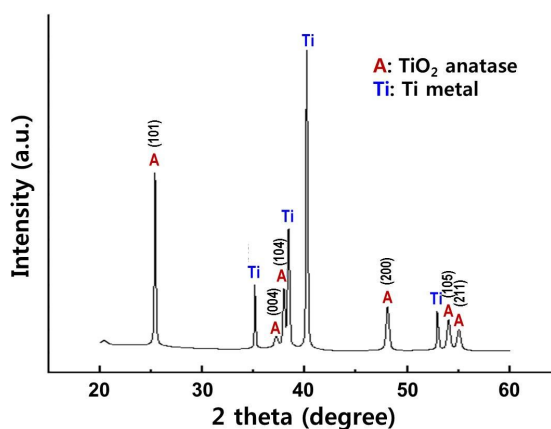


Fig. 4. X-ray diffraction (XRD) spectrum of TiO₂ nanotube arrays on Ti metallic membrane annealed at 500 °C for 1 h.

Fig. 5 shows the temperature of the electrolyte in anodizing bath during anodic oxidation. The sample size and starting temperature of water jacket were 2 × 3 cm² and 30 °C, respectively. The

temperature linearly increased to 34 °C for 20 min. To keep the temperature of 30 °C, the water jacket having a chiller was used for the anodizing bath. The temperature increased faster for the larger areas of Ti metallic membranes.

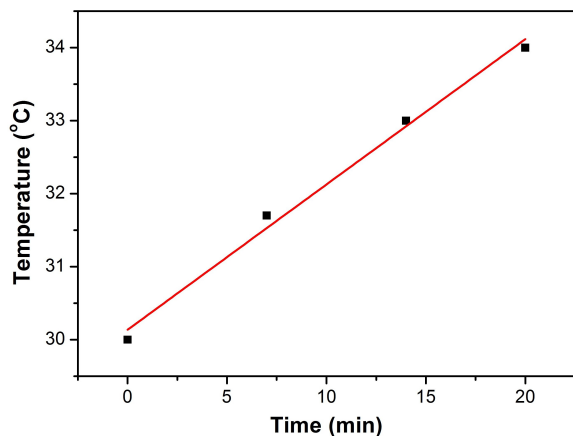


Fig. 5. Temperature of electrolyte in anodizing bath versus anodizing time.

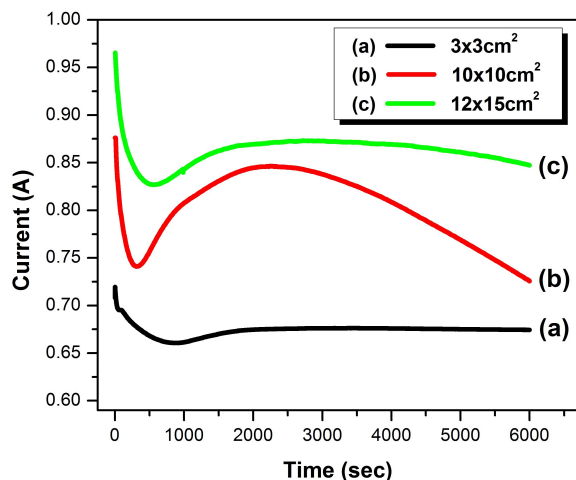


Fig. 6. Transient current versus anodizing time on various areas of $3 \times 3 \text{ cm}^2$, $10 \times 10 \text{ cm}^2$, and $12 \times 15 \text{ cm}^2$.

Fig. 6 shows the transient current versus anodizing time on various areas of $3 \times 3 \text{ cm}^2$, $10 \times 10 \text{ cm}^2$, and $12 \times 15 \text{ cm}^2$. Transient current shapes for all samples correspond to a typical transient current shape observed during anodic oxidation. The value of transient current increased with the area of Ti metallic membrane. Because the large surface area

induced low resistance between Ti metallic membrane as an anode and tantalum as a cathode, high transient current of $\sim 0.9 \text{ A}$ was measured for the $12 \times 15 \text{ cm}^2$ sample. Joule's heat resulting from high transient current quickly raised the temperature of electrolyte. Maintaining an optimal temperature can be a hard challenge in anodic oxidation of large scale Ti metallic membranes.

4. Conclusions

To increase the photocatalytic degradation efficiency on the refractory organic contaminants in water, TiO₂ nanotube arrays on the surface Ti metallic membrane were fabricated by anodic oxidation. Ti metallic membranes with various surface areas were anodized and their microstructures were studied. TiO₂ nanotubes were hexagonally close-packed together and their crystalline phase was changed into the anatase phase by annealing at 500 °C. High transient current of $\sim 0.9 \text{ A}$ was measured for $12 \times 15 \text{ cm}^2$ sample. Joule's heat resulting from the high transient current should be controlled to keep the optimal anodizing temperature. Temperature and transient current were very important factors in anodic oxidation for large scale Ti metallic membrane fabrication.

Acknowledgements

This research was financially supported by the Ministry of Education, Science Technology (MEST) and National Research Foundation of Korea (NRF) through the Human Resource Training Project for Regional Innovation (Grant No. NRF-2015H1C1A1035848 and 2012H1B8A2026009).

References

- [1] RACHEL A., SUBRAHMANYAM M., BOULE P., *Appl. Catal. B-Environ.*, 37 (2002), 301.
- [2] DIONYSIOU D.D., SUIDAN M.T., BEKOU E., BAUDIN I., LAIN J.-M., *Appl. Catal. B-Environ.*, 26 (2000), 153.
- [3] YAMASHITA H., HARADA M., MISAKA J., TAKEUCHI M., NEPPOLIAN B., ANPO M., *Catal. Today*, 84 (2003), 191.
- [4] SAKTHIVEL S., SHANKAR M., PALANICHAMY M., ARABINDOO B., MURUGESAN V., *J. Photoch. Photobiol. A*, 148 (2002), 153.
- [5] CHEN Y., WANG K., LOU L., *J. Photoch. Photobiol. A*, 163 (2004), 281.
- [6] WIESNER M.R., BOTTERO J.-Y., *Environmental Nanotechnology: Applications and Impacts of Nanomaterials*, The McGraw-Hill Companies, New York, 2007.

- [7] KAGAYA S., SHIMIZU K., ARAI R., HASEGAWA K., *Water Res.*, 33 (1999), 1753.
- [8] LEE S.-A., CHOO K.-H., LEE C.-H., LEE H.-I., HYEON T., CHOI W., KWON H.-H., *Ind. Eng. Chem. Res.*, 40 (2001), 1712.
- [9] HONDA R.J., KEENE V., DANIELS L., WALKER S., *J. Environ. Eng. Sci.*, 3 (2014), 127.
- [10] CHUANG Y.-H., HONG G.-B., CHANG C.-T., *J. Air Waste Manage.*, 64 (2014), 738.
- [11] MOLINARI R., MUNGARI M., DRIOLI E., DI PAOLA A., LODDO V., PALMISANO L., SCHIAVELLO M., *Catal. Today*, 55 (2000), 71.
- [12] SCHIAVELLO M., *Photocatalysis and Environment. Trends and Applications*, Kluwer Academic Publishers, Dordrecht, 1988.
- [13] CHOI H., STATHATOS E., DIONYSIOU D.D., *Appl. Catal. B-Environ.*, 63 (2006), 60.
- [14] CHOI W.-Y., CHUNG J., CHO C.-H., KIM J.-O., *Desalination*, 279 (2011), 359.
- [15] PAN G.-T., HUANG C.-M., CHEN L.-C., SHIU W.-T., *J. Environ. Eng. Landsc.*, 16 (2006), 413.
- [16] SHON H., PHUNTSO S., VIGNESWARAN S., *Desalination*, 225 (2008), 235.
- [17] PARAMASIVAM I., MACAK J., SCHMUKI P., *Electrochem. Commun.*, 10 (2008), 71.
- [18] ALBU S.P., GHICOV A., MACAK J.M., HAHN R., SCHMUKI P., *Nano Lett.*, 7 (2007), 1286.
- [19] YANG D.-J., KIM H.-G., CHO S.-J., CHOI W.-Y., *IEEE T. Nanotechnol.*, 7 (2008), 131.
- [20] SHANKAR K., MOR G.K., PRAKASAM H.E., YORIYA S., PAULOSE M., VARGHESE O.K., GRIMES C.A., *Nanotechnology*, 18 (2007), 065707.
- [21] YANG D.-J., KIM H.-G., CHO S.-J., CHOI W.-Y., *Mater. Lett.*, 62 (2008), 775.
- [22] KIM W.-R., PARK H., CHOI W.-Y., *Nanoscale Res. Lett.*, 9 (2014), 1.
- [23] CHOI W.-Y., LEE Y.-W., KIM J.-O., *Res. Chem. Intermediat.*, 39 (2013), 1517.
- [24] CHOI W.-Y., LEE Y.-W., KIM J.-O., *Desalin. Water Treat.*, 34 (2011), 229.
- [25] WANG M., IOCOZZIA J., SUN L., LIN C., LIN Z., *Energy Environ. Sci.*, (2014),
- [26] ZHANG X., CHAI Y., LIN L., ZHANG K., ZHAO B., HE D., *Catal. Lett.*, 144 (2014), 987.

Received 2014-12-09

Accepted 2015-04-21